In situ study of the synthesis of ThSiO$_4$ under environmental representative conditions

Paul Estevenon,[a,b,†] Jeremy Causse,[*a] Stephanie Szenknect,[a] Eleonore Welcomme,[b] Adel Mesbah,[a] Philippe Moisy,[b] Christophe Poinssot [b] and Nicolas Dacheux [a]

[a] ICSM, CEA, CNRS, ENSCM, Univ Montpellier, Site de Marcoule – Bât. 426, BP 17171, 30207 Bagnols-sur-Cèze, France.

[b] CEA, DES, ISEC, DMRC*, Univ Montpellier, Marcoule, France.*

† Present addresses:
The European Synchrotron, CS40220, 38043 Grenoble Cedex 9, France.
Helmholtz Zentrum Dresden-Rossendorf (HZDR), Institute of Resource Ecology, P.O. Box 510119, 01314, Dresden, Germany.

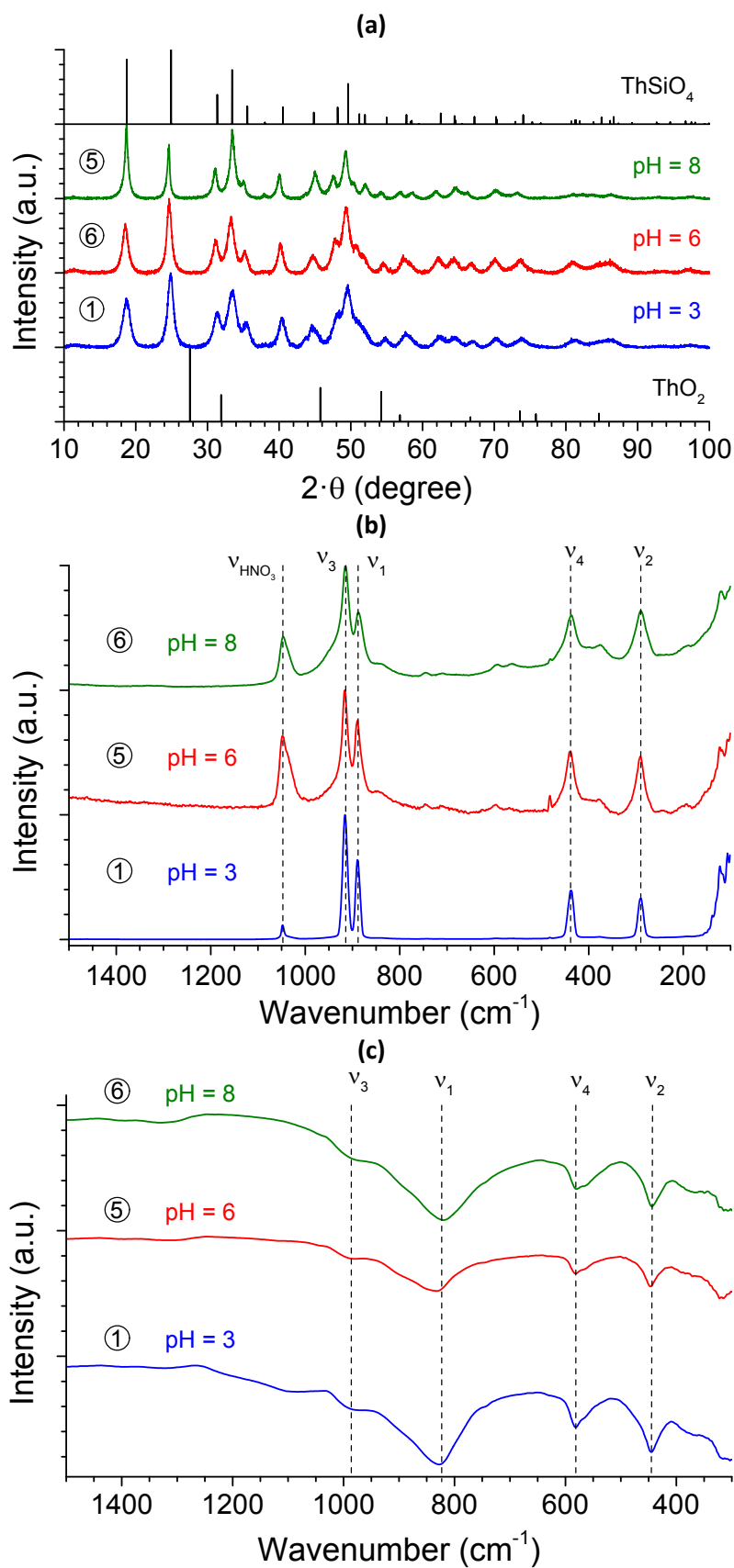**SUPPORTING INFORMATION**

(a)

(b)

(c)

Figure S1. PXRD patterns (a), Raman (b) and infrared spectra (c) obtained for samples prepared with starting silicate and thorium(IV) concentrations of 0.21 mol·L^{-1} in nitric reactive media at 90°C starting with initial pH equal to: 8 (5), 6 (6) and 3 (1). Characteristic XRD lines of ThO$_2$ and ThSiO$_4$ were extracted from references [1] and [2], respectively.
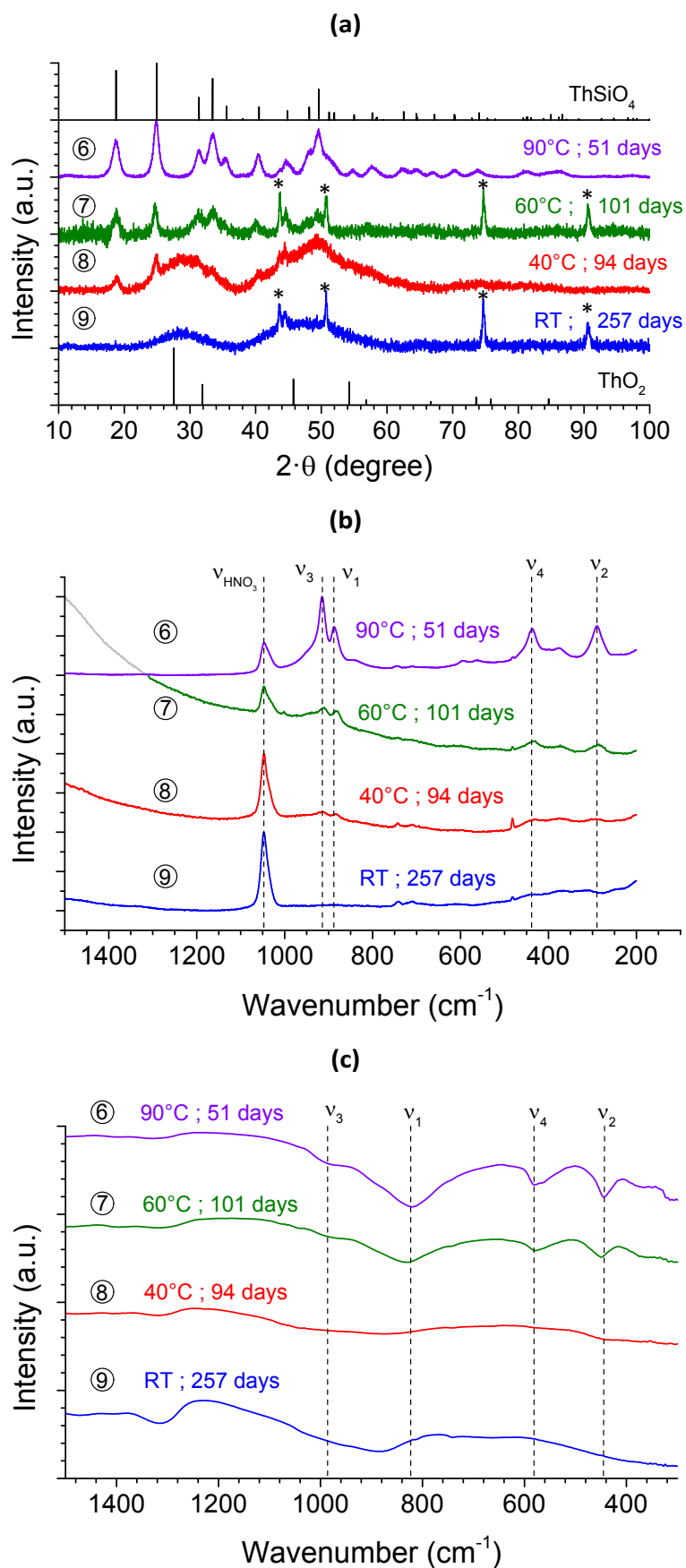
Figure S2. PXRD patterns (a), Raman (b) and infrared spectra (c) obtained for samples prepared with starting silicate and thorium(IV) concentrations of 0.21 mol·L^{-1} in nitric reactive media at initial pH = 6 at 90°C for 51 days (1), 60°C for 101 days (2), 40°C for 94 days (3) and at room temperature for 257 days (4). Characteristic XRD lines of ThO_2 and $ThSiO_4$ were extracted from references [1] and [2], respectively. * is relative to diffraction peaks due to sample holder.
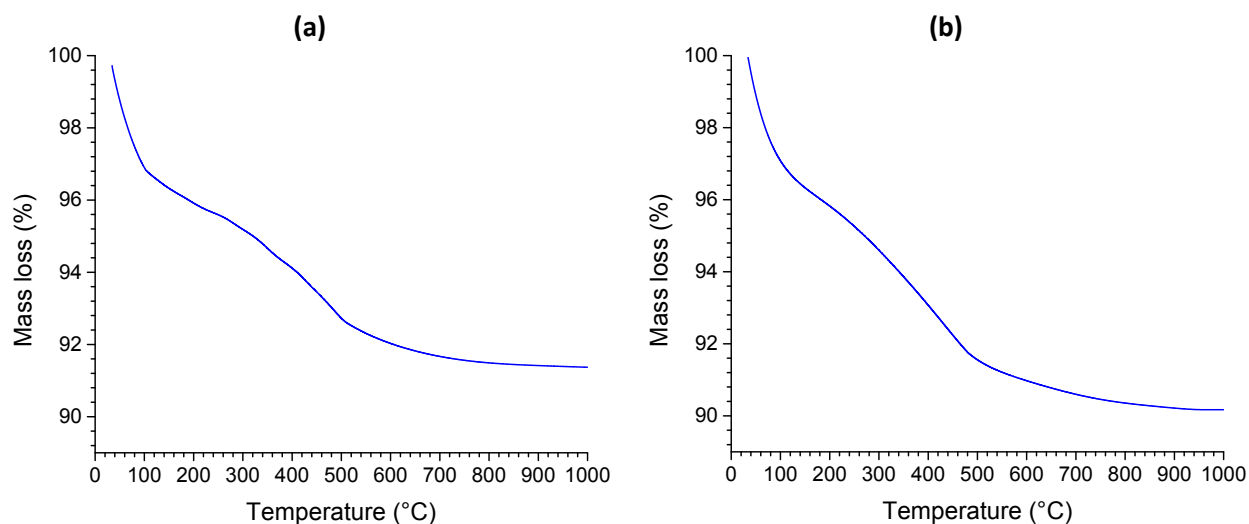
Figure S3. Thermogravimetric analyses performed between room temperature and 1000°C, under air atmosphere, for samples prepared with starting silicate and thorium(IV) concentrations of 0.21 mol·L^{-1} in nitric reactive media at initial pH = 3 at 90°C for 51 days (a), 60°C for 101 days (b)

Figure S4. PXRD patterns obtained for samples prepared with starting silicate and thorium(IV) concentrations of 0.21 mol·L^{-1} in nitric reactive media at initial 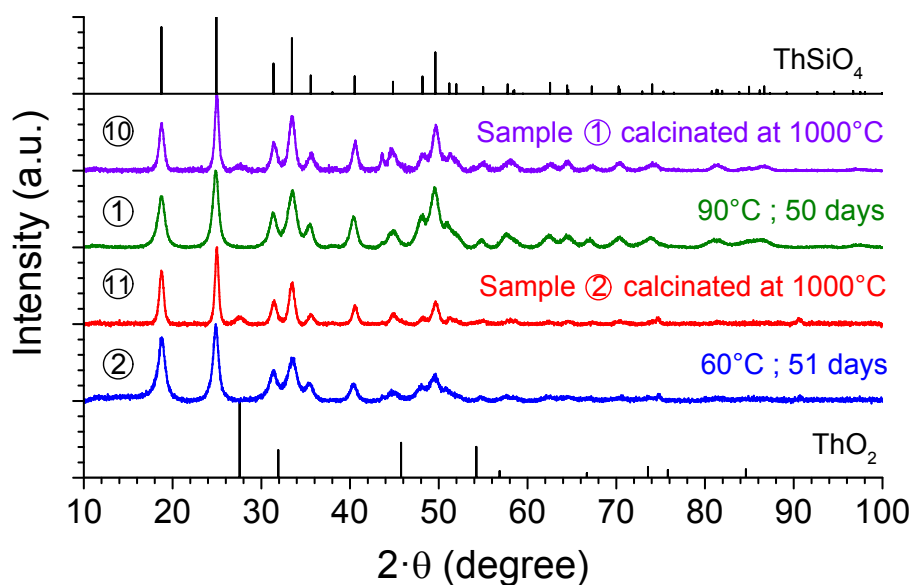pH = 3 at 90°C for 51 days (1), 60°C for 101 days (2) and the samples respectively obtained after thermogravimetric analyses at 1000°C (10) and (11). Characteristic XRD lines of ThO_2 and $ThSiO_4$ were extracted from references [1] and [2], respectively.
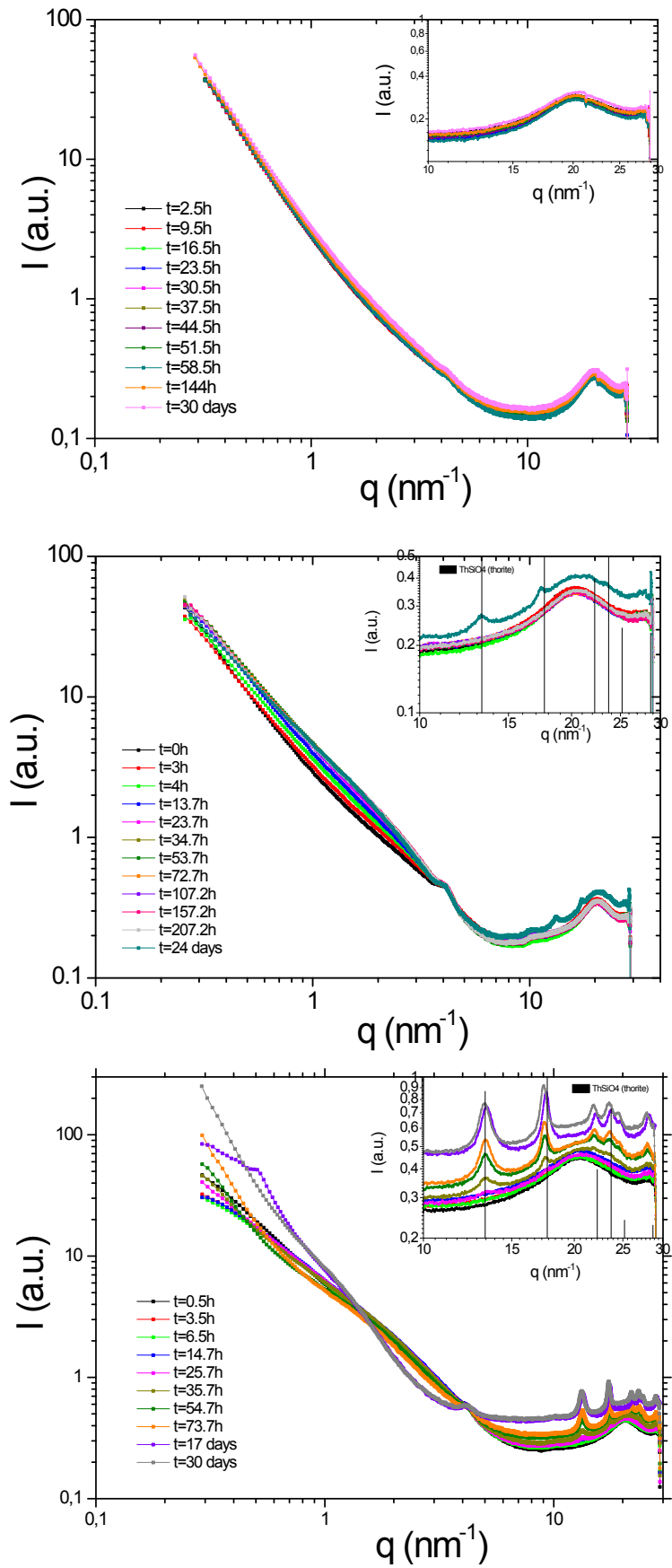
Figure S5. Small and Wide-Angle X-Rays Scattering measurements kinetics at room temperature (RT, top), 40°C (middle) and 60°C (bottom) for pH = 6. Peak around 4.5 nm^{-1} is due to Kapton foils present in the swaxs experimental set-up.

Table S1. Life-times of unaggregated colloids (STEP I); aggregates (STEP II) and for the appearance of $ThSiO_4$ crystals (STEP III) for experiments performed at pH = 6, RT, 40°C and 60°C

	Colloids (STEP I)	**Aggregates (STEP II)**	**$ThSiO_4$ crystals (STEP III)**
pH 6 – RT	Not detected	0 – 30 days	>> 90 days
pH 6 – 40°C	Not detected	0 – 24 days	24 days
pH 6 – 60°C	Not detected	0 – 35.7 h	35.7 h

Table S2. Fitting parameters, cylinder length (L), cylinder radius (R) and standard deviation of cylinder length Gaussian distribution (σ) obtained with SASFit software for the experiments performed at pH = 3.

	time (h)	L (nm)	R (nm)	σ
RT	0,00	3,64	0,47	0,33
	4,50	3,95	0,51	0,95
	8,00	4,40	0,50	0,87
	11,50	4,46	0,53	0,82
	15,00	4,70	0,56	0,83
	18,50	4,75	0,55	0,99
	22,00	5,14	0,54	0,69
	25,50	5,54	0,55	0,75
	29,00	5,59	0,55	0,53
	32,50	5,45	0,56	0,86
	36,00	5,66	0,56	0,61
	39,50	5,61	0,55	0,68
	43,00	5,94	0,56	0,72
	46,50	6,24	0,56	0,60
	50,00	5,86	0,57	0,77
	53,50	6,28	0,55	0,80
	57,00	5,88	0,58	1,14
	60,50	6,30	0,55	0,71
	144,00	9,34	0,62	1,12
	152,00	10,10	0,64	0,76
40°C	0,50	2,39	0,33	0,52
	2,00	2,22	0,40	0,86
	3,50	2,20	0,42	1,10
	5,00	2,61	0,41	1,00
	6,50	2,89	0,42	1,00
	9,67	3,45	0,43	1,00
	14,17	4,00	0,43	1,00
	18,67	4,56	0,43	1,00
	24,17	4,98	0,44	1,00
	29,67	5,18	0,46	1,00
	35,17	6,06	0,45	1,00
	44,67	8,11	0,46	1,00
	54,17	10,14	0,48	1,00
60°C	0	4	0,4	0,85
	1,5	6,5	0,4	0,68
	3	10,4	0,4	0,30

Small-Angle X-Ray scattering treatment:

1 - Cylinder Form Factor:

$$P(q) = \left(\Delta\rho\pi R^2 L\right)^2 \frac{2}{qL}\left[Si_{\frac{\pi}{2}}(qL)\Lambda_1^2(qR) - \frac{\omega(2qR)}{qL} - \frac{\sin(qL)}{(qL)^2}\right]$$

Where:

$$Si_{\frac{\pi}{2}}(qL) = \left(Si(qL) + \frac{\cos(qL)}{qL} + \frac{\sin(qL)}{(qL)^2}\right)$$

$$Si(x) = \int_0^x \frac{\sin t}{t}dt$$

$$\Lambda_1(x) = \frac{2}{x}J_1(x)$$

$$\Lambda_2(x) = \frac{8}{x^2}J_2(x)$$

$$\omega(x) = \frac{8}{x^2}(3J_2(x) + J_0(x) - 1)$$

$J_n(x)$ are the regular cylindrical Bessel functions of order *n*.

With *q*, scattering vector, *R*, the cylinder radius and *L*, the cylinder length, ρ, the electronic scattering length, and Δρ, the scattering contrast.

In order to take into account polydispersity of the scattering objects, a size distribution was applied to cylinder length *L*. This size distribution follows a Gaussian law:

$$G(L, N_{ob}, \sigma, L_0) = \frac{N_{ob}}{\sigma\sqrt{2\pi}}e^{-\frac{(L-L_0)^2}{2\sigma^2}}$$

Where N_{ob} is the number of scattering objects per volume, σ is the standard deviation and L_0 is the mean cylinder length.

2 – Data Fitting

Several form factor models were attempted to describe experimental data points, more particularly cylinder, sphere and spherical core-shell made of respectively thorite in the core and hydrated thorite in the shell.

The goodness of the fits are represented in the figure S7. It is clear that the decrease of scattered intensity in experimental data points is smooth. This smoothness could only be fitted with cylinder form factor model. Spherical models (homogeneous sphere or core shell) always presented strong decrease of the scattered intensity. Therefore, it was not possible to fit experimental data on the whole q range for those spherical models, even if size of sphere, core, shell, or composition of the shell was changed (ratio thorite/water in the shell).
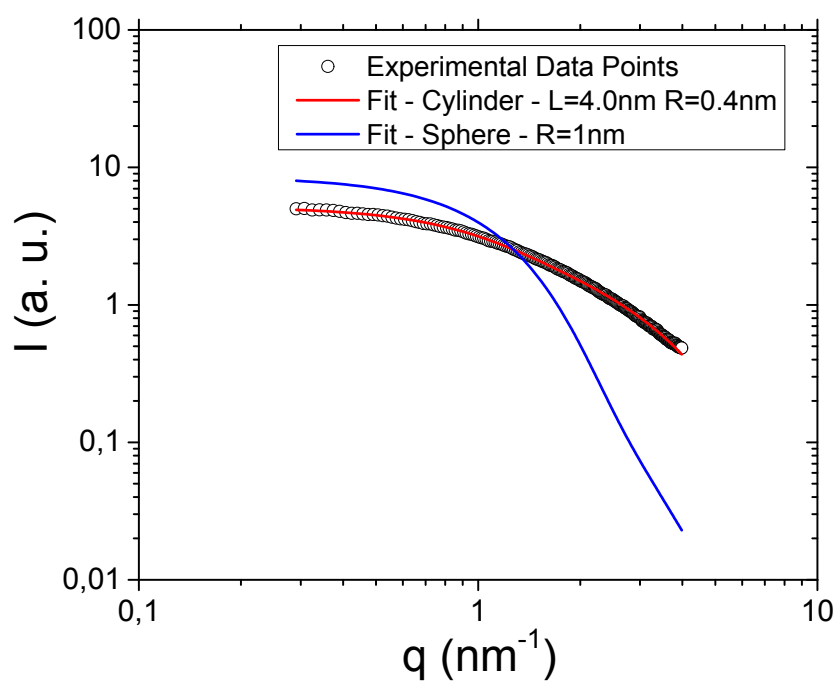
Figure S6. SWAXS experimental data series for system at 60°C, pH=3 and t=0. Comparison of the experimental data series with fits.

References:

1. Holzer, J.; McCarthy, G., Inorganic Crystal Structure Database (ICSD) collection. 1991.
2. Fuchs, L. H.; Gebert, E., X-ray studies of synthetic coffinite, thorite and uranothorites. *The American Mineralogist* **1958,** *43*, 243-248.